American **Heart** Association

American **Stroke** Association®

Age-Related Decline in Oligodendrogenesis Retards White Matter Repair in Mice

Nobukazu Miyamoto, Loc-Duyen D. Pham, Kazuhide Hayakawa, Toshinori Matsuzaki, Ji Hae Seo, Caroline Magnain, Cenk Ayata, Kyu-Won Kim, David Boas, Eng H. Lo and Ken Arai

The online version of this article, along with updated information and services, is located on the
World Wide Web at:
http://stroke.ahajournals.org/content/44/9/2573

Data Supplement (unedited) at:
http://stroke.ahajournals.org/content/suppl/2013/07/23/STROKEAHA.113.001530.DC1.html

Age-Related Decline in Oligodendrogenesis Retards White Matter Repair in Mice

Nobukazu Miyamoto, MD, PhD; Loc-Duyen D. Pham, MS; Kazuhide Hayakawa, PhD;
Toshinori Matsuzaki, MD, PhD; Ji Hae Seo, PhD; Caroline Magnain, PhD;
Cenk Ayata, MD, PhD; Kyu-Won Kim, PhD; David Boas, PhD; Eng H. Lo, PhD; Ken Arai, PhD

Background and Purpose—Aging is one of the major risk factors for white matter injury in cerebrovascular disease. However, the effects of age on the mechanisms of injury/repair in white matter remain to be fully elucidated. Here, we ask whether, compared with young brains, white matter regions in older brains may be more vulnerable in part because of decreased rates of compensatory oligodendrogenesis after injury.

Methods—A mouse model of prolonged cerebral hypoperfusion was prepared by bilateral common carotid artery stenosis in 2-month and 8-month-old mice. Matching in vitro studies were performed by subjecting oligodendrocyte precursor cells to sublethal 7-day $CoCl_2$ treatment to induce chemical hypoxic stress.

Results—Baseline myelin density in the corpus callosum was similar in 2-month and 8-month-old mice. But after induction of prolonged cerebral hypoperfusion, older mice showed more severe white matter injury together with worse deficits in working memory. The numbers of newborn oligodendrocytes and their precursors were increased by cerebral hypoperfusion in young mice, whereas these endogenous responses were significantly dampened in older mice. Defects in cyclic AMP response element-binding protein signaling may be involved because activating cyclic AMP response element-binding protein with the type-III phosphodiesterase inhibitor cilostazol in older mice restored the differentiation of oligodendrocyte precursor cells, alleviated myelin loss, and improved cognitive dysfunction during cerebral hypoperfusion. Cell culture systems confirmed that cilostazol promoted the differentiation of oligodendrocyte precursor cells.

Conclusions—An age-related decline in cyclic AMP response element-binding protein–mediated oligodendrogenesis may compromise endogenous white matter repair mechanisms, and therefore, drugs that activate cyclic AMP response element-binding protein signaling provide a potential therapeutic approach for treating white matter injury in aging brains. (***Stroke***. 2013;44:2573-2578.)

Key Words: aging ■ animal model ■ cyclic AMP response element-binding protein ■ oligodendrocyte ■ white matter diseases

Aging is one of the most important risk factors for developing white matter injury in stroke and cerebrovascular disease.[1] The risk of stroke doubles every decade after 55 years of age,[2] and aged patients show less functional recovery from stroke compared with younger patients.[3] However, the mechanisms that underlie the increased vulnerability of aging white matter remains poorly understood.

Increasingly, it has been proposed that central nervous system pathophysiology is significantly influenced by the balance between deleterious versus beneficial responses to the initial insult.[4] Stroke and brain injury trigger a wide spectrum of neurovascular perturbations, glial activation, neuroinflammation, and neuronal cell death cascades. But many endogenous neuroprotective responses may also be induced at the same time. These include compensatory neurogenesis, angiogenesis, neuroplasticity, and remodeling.[5] Herein may lie a clue to the effects of aging on central nervous system disease. Although the adult brain retains plastic capabilities for regeneration and recovery, aging may significantly dampen these endogenous protective mechanisms. In particular, the capacity for neurogenesis seems to diminish with age. This is primarily because of a general reduction of neuronal precursor cell proliferation because of age-related alterations in the cellular microenvironment: decline of neurotrophic factor expression,[6,7] increase in cell death rate of neuronal precursors and mature neurons,[8] and decrease in the activation of cyclic AMP response element-binding protein (CREB) signaling.[9]

Similar to neurogenesis, oligodendrogenesis and white matter homeostasis might also be affected by white matter senescence.

In healthy young adult brains, myelin-forming mature oligodendrocytes in the white matter can be newly generated from their precursor cells (oligodendrocyte precursor cells [OPCs]). After white matter injury, OPCs rapidly proliferate and migrate to fill the demyelinated area, differentiate into mature oligodendrocytes, and restore myelin sheaths.[10–12] Notably, however, myelin density, along with cognitive function, spontaneously declines with increasing age in both humans and rodents,[13,14] indicating that the capacity for oligodendrogenesis may be associated with white matter senescence. In this study, we ask whether analogous declines in endogenous recovery mechanisms may also occur after central nervous system injury, thus mediating the age-related increase in white matter vulnerability in stroke and cerebrovascular disease.

Methods

Cerebral Prolonged Hypoperfusion Model

All experiments were performed following an institutionally approved protocol in accordance with the National Institutes of Health Guide for the Care and Use of Laboratory Animals. Cerebral prolonged hypoperfusion stress was induced by bilateral common carotid artery stenosis. Male C57Bl/6 mice (2 months and 8 months old; Charles River Institute) were anesthetized with 4.0% isoflurane and then maintained on 1.5% isoflurane in 70% N_2O and 30% O_2 using a small-animal anesthesia system. Through a midline cervical incision, both common carotid arteries were exposed. A microcoil with a diameter of 0.18 mm (Sawane Spring Co) was applied to bilateral common carotid arteries, maintaining the rectal temperature between 36.5°C and 37.5°C using a heating pad. All experimental groups were randomized, and investigators responsible for surgical procedures or drug treatments were blinded. End point assessments (please see online-only Data Supplement for detailed methods of end point assessments) were performed by investigators blinded to the groups to which each animal was assigned.

Cell Culture

OPC cultures were prepared from rat neonatal cortex. Cultured OPCs were plated and maintained in Neurobasal medium containing glutamine, 1% penicillin/streptomycin, 10 ng/mL platelet-derived growth factor, 10 ng/mL fibroblast growth factor, and 2% B27 supplement onto poly-DL-ornithine–coated plates. Four to 5 days after plating, the OPCs were used for the experiments. To differentiate OPCs from myelin basic protein–positive oligodendrocytes, the culture medium was switched to Dulbecco's Modified Eagle Medium containing 1% penicillin/streptomycin, 10 ng/mL ciliary neurotrophic factor, 50 ng/mL T3, and 2% B27 supplement. To mimic chronic mild-hypoxic condition, OPCs were incubated with nonlethal $CoCl_2$ (Sigma). Please see online-only Data Supplement for detailed methods of in vitro cell culture experiments.

Statistical Analysis

On the basis of published and pilot data, power estimates were calculated based on α=0.05 and β=0.8 to obtain group sizes appropriate for detecting effect sizes in the range of 30% to 50% for in vivo models and 40% to 50% for cell culture models. A 1-way ANOVA followed by post hoc Fisher protected least significant difference test was used to determine the significant differences in various indices among the groups. A *P* value of <0.05 was considered statistically significant.

Results

Eight-Month-Old Mice Suffer More White Matter Injury Than 2-Month-Old Mice After Prolonged Cerebral Hypoperfusion

There were no clear differences in myelination and white matter integrity of the corpus callosum in young 2-month-old

mice compared with older 8-month-old mice (Figure S1 in the online-only Data Supplement). We then asked whether in spite of similar baseline conditions, older white matter would still be more vulnerable to injury. Mice were subjected to a standard model of prolonged cerebral hypoperfusion by using microcoils to bilaterally narrow the luminal diameters of their common carotid arteries. There were no initial differences in carotid diameters (2-month-old mice: 341.4±24.6 µm; 8-month-old mice: 342.4±24.7 µm), and the surgical procedures produced similar degrees of cerebral hypoperfusion (2-month-old: 75.9±8.7%; 8-month-old: 78.0±6.6%, cerebral blood flow levels at 14 days relative to sham-operative animals).

For 14 days after onset of cerebral hypoperfusion, white matter integrity was assessed with fluoromyelin staining, myelin basic protein Western blot, and spectral domain optical coherence microscopy imaging (Figure S2 in the online-only Data Supplement). As expected, cerebral hypoperfusion induced a progressive degradation of white matter integrity in the corpus callosum in all mice. But loss of myelin immunostaining (Figure 1A) and myelin basic protein Western blot (Figure 1B) was more severe in older 8-month-old brains compared with the younger 2-month-old brains. Spectral domain optical coherence microscopy imaging confirmed that the 8-month-old brains showed increased myelin fiber derangement and white matter vacuoles (Figure 1C). Consistent with these morphological end points, 8-month-old mice demonstrated more severe neurological deficits compared with younger 2-month-old mice, as measured with the standard Y-maze test. At prehypoperfusion baseline conditions, all
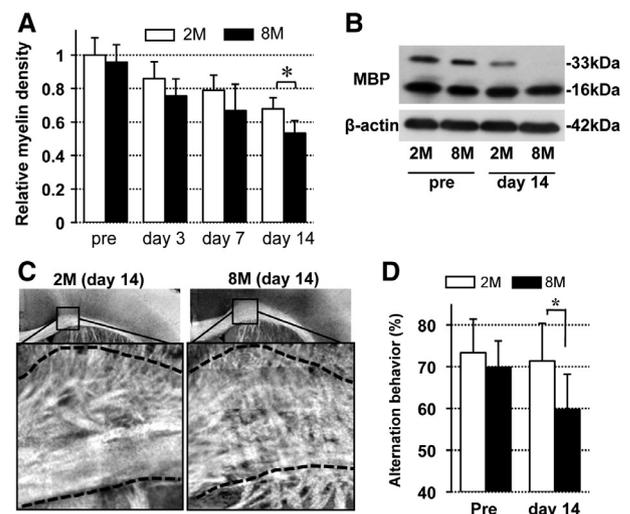
Figure 1. White matter lesion after prolonged cerebral hypoperfusion. **A,** Relative density of fluoromyelin intensity in mouse corpus callosum. Values were calculated based on the density of pretreatment in 2-month-old mice (n=5). **B,** Western blot images for myelin basic protein expression in mouse corpus callosum before and 14 days after the stress onset. β-Actin is an internal control. **C,** Spectral domain optical coherence microscopy images of corpus callosum in 2-month-old and 8-month-old mice at day 14 after white matter injury. **D,** Alternation behavior (index of working/spatial memory) of 2-month and 8-month-old mice at pretreatment and day 14 after injury (n=10). Values are mean±SD (*P<0.05). 2M indicates 2-month-old mice; and 8M, 8-month-old mice.

mice showed normal Y-maze function. But after 2 weeks of cerebral hypoperfusion, Y-maze function was more severely affected in the older 8-month-old mice (Figure 1D).

Eight-Month-Old Mice Show Decreased Oligodendrogenesis After Prolonged Cerebral Hypoperfusion

To assess the hypothesis that older brains possess dampened endogenous repair capacities, we used 5-bromodeoxyuridine (BrdU) incorporation experiments to ask whether oligodendrogenesis is suppressed in aging white matter (Figure S3 in the online-only Data Supplement). In young 2-month-old white matter, the number of BrdU-incorporated cells was increased after cerebral hypoperfusion (Figure 2A). In older 8-month-old white matter, the increase in BrdU-incorporated cells was detectable but significantly reduced compared with 2-month-old white matter (Figure 2A). Double-immunofluorescence labeling with cell-specific markers revealed that the major cell type of BrdU-incorporated cells comprised NG2-positive OPCs in both groups (Table S1 in the online-only Data Supplement).

To confirm these findings, immunostaining was used to quantify the number of NG2 positive OPCs up to 14 days after cerebral hypoperfusion onset. In young 2-month-old brains, the number of NG2-positive OPCs in the corpus callosum was gradually increased over the course of prolonged hypoperfusion (Figure 2B and 2C). In contrast, older 8-month-old brains did not show a significant increase in OPC numbers over time (Figure 2B and 2C). The ratio of single stranded DNA/NG2–double-positive cells (damaged OPCs) at day 14 was significantly larger in the 8-month-old brains (Figure 2D), consistent
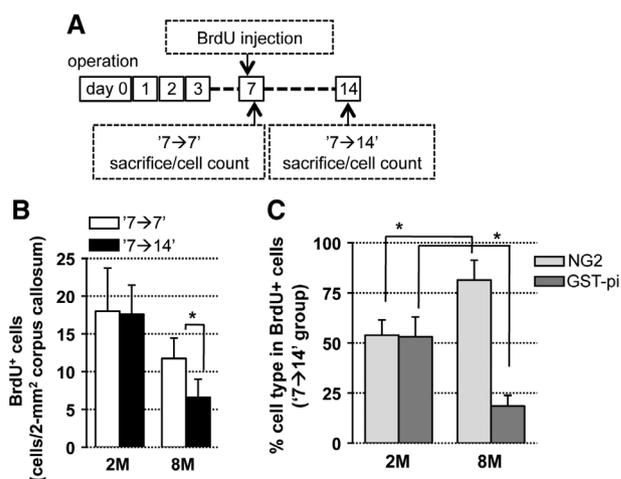
with the observation that OPC numbers did not increase in this older group of mice.

If there is a difference in OPC response in older brains, does this mean that the numbers of mature oligodendrocytes would also be different? To answer this question, 2 BrdU treatment schedules were used: (1) BrdU was injected on day 7 after the hypoperfusion onset, and brains were removed and examined on the same day ('7→7'), and (2) BrdU was injected on day 7, and brains were examined 1 week later ('7→14'; Figure 3A). In young 2-month-old mice, the number of BrdU-positive cells on day 14 was similar to that on day 7 (Figure 3B). In contrast, for 8-month-old mice, the number of BrdU-positive cells on day 14 was less than that on day 7 (Figure 3B), indicating that newly generated OPCs after hypoperfusion in the older brains would die in 1 week without maturing into oligodendrocytes. Double-immunofluorescence labeling with cell-specific markers showed that some of newly generated OPCs on day 7 were successfully differentiated into mature oligodendrocytes on day 14 in young mice. But the older 8-month-old mice did not show equivalent levels of oligodendrogenesis (Figure 3C), indicating that OPCs in the older mice would die before differentiating into mature oligodendrocytes.

CREB Signaling Is Involved in Oligodendrogenesis After White Matter Injury

Older white matter regions may have a dampened recovery response to prolonged cerebral hypoperfusion compared with young brains. To this point, our findings suggest that this may be partly because of a decline in the endogenous capacity for compensatory oligodendrogenesis. But what mechanisms are involved? Because CREB signaling is known to be generally important for neurogenesis and oligodendrogenesis, we asked whether differences in CREB responses may also be involved in our models. Immunostaining showed that, in both young

Figure 2. Oligodendrocyte precursor cell proliferation in vivo. **A**, Number of 5-bromodeoxyuridine (BrdU)-positive (BrdU⁺) cells in the corpus callosum (n=5). **B**, Representative images of NG2 staining in the lateral side of corpus callosum at day 14 after white matter injury (bar=50 μm). **C**, Number of NG2-positive (NG2⁺) cells in mouse corpus callosum during white matter damage (n=5). **D**, Ratio of single-stranded DNA (ssDNA)/NG2–double-positive cells in total NG2 cells in the mouse corpus callosum at day 14 (n=5). 2M indicates 2-month-old mice; and 8M, 8-month-old mice.

Figure 3. Oligodendrocyte precursor cell differentiation in vivo. **A**, Experimental schedule to assess cell differentiation in the corpus callosum using 5-bromodeoxyuridine (BrdU). **B**, Number of BrdU-positive (BrdU⁺) cells in corpus callosum at days 7 and 14 (n=5). **C**, Ratio of BrdU/NG2- and BrdU/GST-π–double-labeled cells in total BrdU cells in corpus callosum at day 14 (BrdU injection: day 7; n=5). Values are mean±SD (*P<0.05). GST-π indicates glutathione S-transferase-π; 2M, 2-month-old mice; and 8M, 8-month-old mice.

and older white matter, phosphorylated CREB signaling was observed in mature oligodendrocytes (CNPase-positive) and OPCs (platelet-derived growth factor receptor-α–positive) under normal conditions, but phosphorylated CREB was primarily expressed within OPCs (Figure 4A; Figure S4 in the online-only Data Supplement). After prolonged cerebral hypoperfusion, phospho-CREB signals decreased in both groups, with a larger reduction present in the 8-month-old brains (Figure 4B and 4C). Western blots confirmed that CREB phosphorylation was significantly lower in 8-month-old brains compared with 2-month-old brains (Figure 4D).
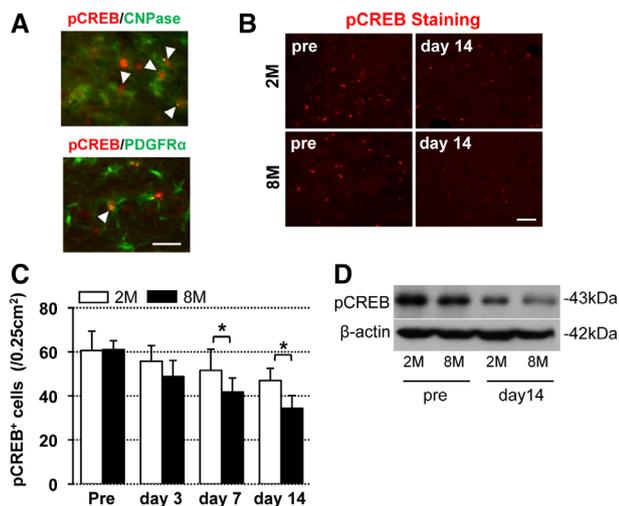
PDE III Inhibitor Cilostazol Promoted OPC Differentiation In Vitro and Rescued OPC Recovery In Vivo

Differences in CREB-mediated OPC proliferation and differentiation may, in part, explain why older white matter was more vulnerable to prolonged cerebral hypoperfusion. So we next asked whether promoting CREB signaling with the phosphodiesterase (PDE) III inhibitor cilostazol could restore these compensatory OPC responses after prolonged stress and injury. To answer this question, we performed both cell culture and in vivo experiments.

First, primary OPCs were cultured from rat neonatal brain cortex. Under normal growth conditions, these OPCs matured over 7 days and decreased the expression of NG2, a marker for OPCs. In contrast, glutathione S-transferase-π and myelin basic protein expression were increased (Figure 5A), indicating that our cultured OPCs successfully differentiated into mature oligodendrocytes in this model system. To mimic the hypoxic

state of prolonged cerebral hypoperfusion, OPCs were treated with 0.01 to 1 μM of $CoCl_2$ for 7 days. As expected, 7 days of $CoCl_2$ treatment increased hypoxia-inducible factor 1-α expression in our cultured OPCs in a dose-dependent manner (Figure 5A). CREB signaling may also be involved as the phosphorylation level of CREB was also decreased by $CoCl_2$-induced chemical hypoxia (Figure 5A). Correspondingly, OPC maturation was inhibited by the chronic $CoCl_2$ treatment (Figure 5A). Lactate dehydrogenase assays showed that 0.01 to 1 μM of $CoCl_2$ did not induce cell death in our OPCs (Figure 5B), indicating that the reduction of OPC maturation by $CoCl_2$ was not merely because of cell death. Next, we asked whether activating CREB with cilostazol could rescue OPC maturation after prolonged chemical hypoxia. Cilostazol alone did not change OPC state (Figure S5 in the online-only Data Supplement) but significantly increased CREB phosphorylation and promoted OPC differentiation under $CoCl_2$-induced hypoxic conditions (Figure 5C and 5D; Figure S5 in the online-only Data Supplement).

Finally, we turned back to our in vivo model of prolonged cerebral hypoperfusion. Cilostazol treatment (10 mg/kg per day for 14 days) was performed by intraperitoneal injection in 8-month-old mice subjected to cerebral hypoperfusion. This treatment schedule was previously reported to effectively inhibit PDE III in brain in vivo.[15] As expected, mice treated with cilostazol showed larger numbers of phopho-CREB–positive cells than the vehicle-treated group did at day 14 (Figure S6 in the online-only Data Supplement). Correspondingly, the cilostazol-treated mice exhibited less white matter injury (Figure 6A; Figure S6 in the online-only Data Supplement), larger number of OPCs (Figure 6B; Figure S6 in the online-only Data Supplement), and better cognitive function (Figure 6C). The BrdU-incorporation/differentiation assay (Figure S7 in the online-only Data Supplement) revealed that cilostazol promoted the proliferation of white matter cells (Figure S8 in the online-only Data Supplement), as well as differentiation of OPCs into mature oligodendrocytes (Figure 6D).

Discussion

Demyelination and cognitive decline are major pathological hallmarks of ischemic white matter diseases, which are mostly associated with increasing age. Although adult brains retain neuroplasticity and regenerative capacities to compensate for lost brain cells, aged brains tend to slowly lose these endogenous repair systems. Our current study demonstrated that white matter regions in aging 8-month-old mice are more vulnerable to prolonged cerebral hypoperfusion, and this is caused in part by a loss of endogenous CREB-mediated oligodendrogenesis. Therefore, drugs that can activate protein kinase A-CREB signaling cascade may provide novel therapeutic approaches for white matter injury in vascular dementia and stroke.

Aging lowers the endogenous capacities for brain regeneration and remodeling. Past studies have demonstrated that aging reduces the differentiation of neuronal precursor cells into neuronal phenotypes,[16] increases the number of dying/dead brain cells,[17] and decreases CREB activation in neurons.[18] Our current data may expand these findings—the capability
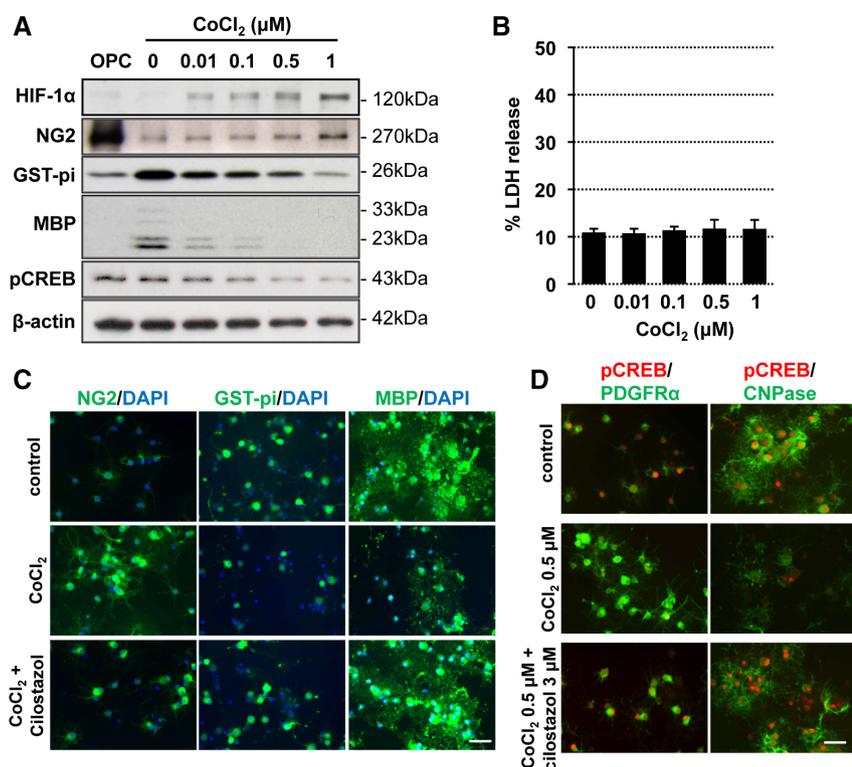
Figure 4. Phospho-CREB (pCREB) in white matter in vivo. **A**, Double immunofluorescent staining of pCREB with CNPase (a marker for mature oligodendrocytes) or PDGFRα (a marker for oligodendrocyte precursor cells) in 2-month-old mice under normal conditions. Arrowheads are double-positive cells (bar=25 μm). **B**, Representative images of pCREB staining in the lateral side of corpus callosum (bar=50 μm). **C**, Number of pCREB-positive (pCREB+) cells in the lateral side of corpus callosum during the hypoperfusion stress (n=5). **D**, Western blot image of pCREB expression in the corpus callosum. β-Actin is an internal control. Values are mean±SD (*P<0.05). CREB indicates cyclic AMP response element-binding protein; PDGFRα, platelet-derived growth factor receptor-α; 2M, 2-month-old mice; and 8M, 8-month-old mice.

Figure 5. Cilostazol-induced OPC proliferation/differentiation in vitro. **A**, Western blot images using samples from cultured rat OPCs with 7-day CoCl$_2$ treatment. HIF-1α is a marker for hypoxic conditions, NG2 is a marker for OPCs, GST-π and MBP are markers for mature oligodendrocytes, and β-actin is an internal control. **B**, LDH assays showed that 0.01 to 1 μM of CoCl$_2$ (7-day treatment) did not induce cell death in our OPCs (n=6). Values are mean±SD. **C**, Representative images of NG2, GST-π, and MBP staining in cultured rat OPCs at day 7 after the CoCl$_2$ treatment with or without cilostazol (bar=25 μm). **D**, Representative images of pCREB, PDGFR-α, and CNPase staining in cultured rat OPCs at day 7 after CoCl$_2$ treatment with or without cilostazol (bar=25 μm). DAPI indicates 4',6-diamidino-2-phenylindole; GST-π, glutathione S-transferase-π; HIF-1α, hypoxia-inducible factor 1-α; LDH, lactate dehydrogenase; MBP, myelin basic protein; OPC, oligodendrocyte precursor cells; and pCREB, phosphorylated cyclic AMP response element-binding protein.

of oligodendrogenesis in the white matter also decreases with aging through deactivation of CREB signaling. In this study, middle-aged mice showed lower phospho-CREB level in the white matter than young mice under pathological conditions. Moreover, activating CREB by a PDE III inhibitor cilostazol alleviated the white matter dysfunction in middle-aged mice by protecting newly generated OPCs and enhancing OPC proliferation/maturation. Cilostazol has been approved for the treatment of intermittent claudication and has been shown to improve pain-free walking distance worldwide in patients with peripheral arterial disease[19] and help in the secondary prevention of ischemic stroke in Japan.[20] Our findings provide initial proof-of-concept that cilostazol (or other PDE III inhibitors) might be a promising drug for age-related white matter diseases. But of course, more extensive preclinical studies are required before this approach can be translated into clinical applications.

Although our current findings demonstrate that aged white matter possesses less capacity for oligodendrogenesis, many important caveats remain. First, we focused on only oligodendrocyte lineage cells in this study. But there are other cell types in white matter, including endothelial cells and astrocytes. The concept of the neurovascular unit suggests that interactions between different cell types maintain brain function under normal conditions and facilitates brain remodeling after injury in the gray matter.[5] In white matter, cell–cell trophic coupling might similarly participate in white matter homeostasis. Indeed, both cerebral endothelial cells and astrocytes show supportive effects for oligodendrocytes/OPCs.[21] Hence, future studies should examine whether the trophic coupling between oligodendrocytes and neighboring cells diminishes with aging in the white matter. Second, our current study demonstrates that loss of CREB activation in the aging
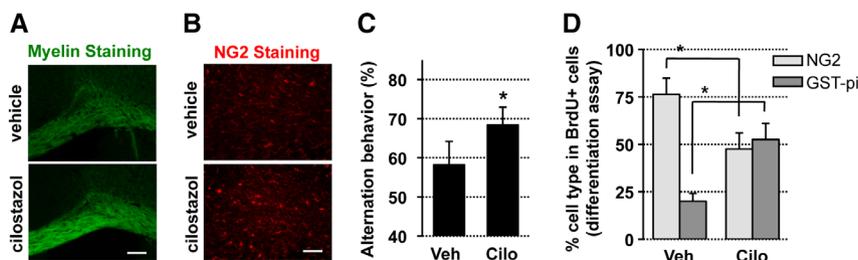
Figure 6. Cilostazol-induced white matter repair in middle-aged mice. **A**, Representative images of fluoromyelin staining in 8-month-old mice with or without cilostazol treatment at day 14 (bar=100 μm). Quantitative data are shown in Figure S6D in the online-only Data Supplement. **B**, Representative images of NG2 staining in the lateral side of corpus callosum in 8-month-old mice with or without cilostazol (10 mg/kg per day for 14 days, IP) at day 14 after white matter injury (bar=50 μm). Quantitative data are shown in Figure S6E in the online-only Data Supplement. **C**, Alternation behavior (index of working/spatial memory) of 8-month-old mice with or without cilostazol treatment at day 14 (n=8). **D**, Ratio of BrdU/NG2- and BrdU/GST-π–double-labeled cells in total BrdU cells in 8-month-old mice corpus callosum at day 14 (n=5). Values are mean±SD. *$P<0.05$. Experimental schedule for the oligodendrocyte precursor cells differentiation assay is shown in Figure S7 in the online-only Data Supplement. BrdU indicates 5-bromodeoxyuridine; Cilo, cilostazol-treatment group; GST-π, glutathione S-transferase-π; and Veh, vehicle group.

8-month-old white matter leads to deficits in oligodendrogenesis. But what factors/mechanisms lower the CREB signaling in the middle-aged white matter? CREB activation is regulated by several growth factors, such as brain-derived neurotrophic factor, and growth factor expressions are decreasing in aging.[22] Hence, reduction of growth factor expression may fail the CREB activation during the stress in aged white matter. These questions should be explored in future studies. Finally, it is important to acknowledge that trying to correlate aging mouse models to the aging human brain is not straightforward. To date, most aging studies with rodents have focused on differences between young (2–3 months old) and very old (>12–15 months old) brains.[23] But it might be possible that the age-related decline in oligodendrogenesis would occur even before obvious declines in myelin density or cognitive function. In this study, we compared young 2-month-old mice with older 8-month mice. It is possible that our models may mimic middle-aged humans. But further studies are warranted to carefully track the temporal profile of these CREB-mediated mechanisms in a wider age range of mice.

In conclusion, our current study demonstrates novel mechanisms by which aging white matter in mouse brain is more vulnerable to prolonged cerebral hypoperfusion and hypoxic stress. Importantly, these phenomena occurred in mice that had normal myelin density and cognitive function at baseline; no deficits were present yet. But these aging regions had lost their ability to recruit CREB-mediated oligodendrogenesis for responding to injury and stress. Hence, drugs that can activate CREB signaling may be a promising approach for aging patients with white matter–related diseases such as vascular dementia or stroke.

Please see online-only Data Supplement for methods and additional data.

Sources of Funding

Disclosures

None.

References

1. Gorelick PB, Scuteri A, Black SE, Decarli C, Greenberg SM, Iadecola C, et al; American Heart Association Stroke Council; Council on Epidemiology and Prevention; Council on Cardiovascular Nursing; Council on Cardiovascular Radiology and Intervention; Council on Cardiovascular Surgery and Anesthesia. Vascular contributions to cognitive impairment and dementia: a statement for healthcare professionals from the American Heart Association/American Stroke Association. *Stroke*. 2011;42:2672–2713.

2. Marini C, Triggiani L, Cimini N, Ciancarelli I, De Santis F, Russo T, et al. Proportion of older people in the community as a predictor of increasing stroke incidence. *Neuroepidemiology*. 2001;20:91–95.

3. Béjot Y, Rouaud O, Jacquin A, Osseby GV, Durier J, Manckoundia P, et al. Stroke in the very old: incidence, risk factors, clinical features, outcomes and access to resources–a 22-year population-based study. *Cerebrovasc Dis*. 2010;29:111–121.

4. Lo EH. A new penumbra: transitioning from injury into repair after stroke. *Nat Med*. 2008;14:497–500.

5. Moskowitz MA, Lo EH, Iadecola C. The science of stroke: mechanisms in search of treatments. *Neuron*. 2010;67:181–198.

6. Kaplan MS, Bell DH. Mitotic neuroblasts in the 9-day-old and 11-month-old rodent hippocampus. *J Neurosci*. 1984;4:1429–1441.

7. Kuhn HG, Dickinson-Anson H, Gage FH. Neurogenesis in the dentate gyrus of the adult rat: age-related decrease of neuronal progenitor proliferation. *J Neurosci*. 1996;16:2027–2033.

8. Walter J, Keiner S, Witte OW, Redecker C. Age-related effects on hippocampal precursor cell subpopulations and neurogenesis. *Neurobiol Aging*. 2011;32:1906–1914.

9. Asanuma M, Nishibayashi S, Iwata E, Kondo Y, Nakanishi T, Vargas MG, et al. Alterations of cAMP response element-binding activity in the aged rat brain in response to administration of rolipram, a cAMP-specific phosphodiesterase inhibitor. *Brain Res Mol Brain Res*. 1996;41:210–215.

10. Miyamoto N, Tanaka R, Shimura H, Watanabe T, Mori H, Onodera M, et al. Phosphodiesterase III inhibition promotes differentiation and survival of oligodendrocyte progenitors and enhances regeneration of ischemic white matter lesions in the adult mammalian brain. *J Cereb Blood Flow Metab*. 2010;30:299–310.

11. Skihar V, Silva C, Chojnacki A, Döring A, Stallcup WB, Weiss S, et al. Promoting oligodendrogenesis and myelin repair using the multiple sclerosis medication glatiramer acetate. *Proc Natl Acad Sci USA*. 2009;106:17992–17997.

12. Gensert JM, Goldman JE. Endogenous progenitors remyelinate demyelinated axons in the adult CNS. *Neuron*. 1997;19:197–203.

13. Doucette JR, Jiao R, Nazarali AJ. Age-related and cuprizone-induced changes in myelin and transcription factor gene expression and in oligodendrocyte cell densities in the rostral corpus callosum of mice. *Cell Mol Neurobiol*. 2010;30:607–629.

14. Sim FJ, Zhao C, Penderis J, Franklin RJ. The age-related decrease in CNS remyelination efficiency is attributable to an impairment of both oligodendrocyte progenitor recruitment and differentiation. *J Neurosci*. 2002;22:2451–2459.

15. Tanaka Y, Tanaka R, Liu M, Hattori N, Urabe T. Cilostazol attenuates ischemic brain injury and enhances neurogenesis in the subventricular zone of adult mice after transient focal cerebral ischemia. *Neuroscience*. 2010;171:1367–1376.

16. Kempermann G, Kuhn HG, Gage FH. Experience-induced neurogenesis in the senescent dentate gyrus. *J Neurosci*. 1998;18:3206–3212.

17. Lemaire V, Koehl M, Le Moal M, Abrous DN. Prenatal stress produces learning deficits associated with an inhibition of neurogenesis in the hippocampus. *Proc Natl Acad Sci USA*. 2000;97:11032–11037.

18. Charalampopoulos I, Alexaki VI, Tsatsanis C, Minas V, Dermitzaki E, Lasaridis I, et al. Neurosteroids as endogenous inhibitors of neuronal cell apoptosis in aging. *Ann N Y Acad Sci*. 2006;1088:139–152.

19. Barnett AH, Bradbury AW, Brittenden J, Crichton B, Donnelly R, Homer-Vanniasinkam S, et al. The role of cilostazol in the treatment of intermittent claudication. *Curr Med Res Opin*. 2004;20:1661–1670.

20. Shinohara Y, Katayama Y, Uchiyama S, Yamaguchi T, Handa S, Matsuoka K, et al; CSPS 2 Group. Cilostazol for prevention of secondary stroke (CSPS 2): an aspirin-controlled, double-blind, randomised non-inferiority trial. *Lancet Neurol*. 2010;9:959–968.

21. Arai K, Lo EH. Oligovascular signaling in white matter stroke. *Biol Pharm Bull*. 2009;32:1639–1644.

22. Rage F, Silhol M, Binamé F, Arancibia S, Tapia-Arancibia L. Effect of aging on the expression of BDNF and TrkB isoforms in rat pituitary. *Neurobiol Aging*. 2007;28:1088–1098.

23. Popa-Wagner A, Buga AM, Kokaia Z. Perturbed cellular response to brain injury during aging. *Ageing Res Rev*. 2011;10:71–79.

SUPPLEMENTAL MATERIAL

Age-related decline in oligodendrogenesis retards white matter repair in mice

Nobukazu Miyamoto[1], Loc-Duyen D. Pham[1], Kazuhide Hayakawa[1], Toshinori Matsuzaki[1], Ji Hae Seo[1,4], Caroline Magnain[2], Cenk Ayata[3], Kyu-Won Kim[4], David Boas[2], Eng H. Lo[1], Ken Arai[1]

[1]Neuroprotection Research Laboratory. Departments of Radiology and Neurology, Massachusetts General Hospital and Harvard Medical School, USA.

[2]Athinoula A. Martinos Center for Biomedical Imaging, Department of Radiology, Massachusetts General Hospital and Harvard Medical School, USA.

[3]Neurovascular Research Laboratory, Department of Radiology, Massachusetts General Hospital and Harvard Medical School, USA.

[4]NeuroVascular Coordination Research Center, College of Pharmacy and Research Institute of Pharmaceutical Sciences, Seoul National University, Seoul 151-742, Korea.

Corresponding author: Ken Arai, Neuroprotection Research Laboratory, MGH East 149-2401, Charlestown, MA 02129, USA. Tel: 617.724.9503, Email: karai@partners.org

Contents:
 - Supplemental Methods
 - Supplemental Table
 - Supplemental Figures and Figure Legends
 - Supplemental References

1

Supplemental Methods:

Cerebral prolonged hypoperfusion model - All experiments were performed following an institutionally approved protocol in accordance with the National Institutes of Health Guide for the Care and Use of Laboratory Animals. Cerebral prolonged hypoperfusion stress was induced by bilateral common carotid artery stenosis (BCAS). Male C57Bl/6 mice (2 and 8 months old, Charles River Institute) were anesthetized with 4.0% isoflurane and then maintained on 1.5% isoflurane in 70% N_2O and 30% O_2 using a small-animal anesthesia system. Through a midline cervical incision, both common carotid arteries were exposed. A microcoil with a diameter of 0.18 mm (Sawane Spring Co.) was applied to bilateral common carotid arteries [4], maintaining the rectal temperature between 36.5°C and 37.5°C using heating pad. Mice were divided at random into four groups: (i) BCAS group (n=60), (ii) BCAS with vehicle treatment group (n=20) - mice in this group received an ip of 0.5% CMC, (iii) BCAS with cilostazol treatment group (n=20) - mice in this group received intraperitoneal injections of 10 mg/kg/day cilostazol (Sigma) suspended in 0.5% carboxymethyl cellulose sodium salt (CMC) (Sigma), every day until the analysis, and (iv) Control sham-operated groups (n=10) - mice in the control group were sham-operated, which involved bilateral exposure of the common carotid arteries. To image common carotid artery (CCA), endothelial cells were labeled by lectin-tomato (Vector laboratory). Lectin (0.2 mg/ml, 400μl) was injected through jugular vein, and then CCA area was analyzed with a fluorescence microscope (Olympus BX51) interfaced with a digital charge-coupled device camera and an image analysis system. To analysis for cerebral blood flow (CBF), a solution of yellow-green fluospheres (15 ± 0.5 μm diameter, 1,000,000 fluorescent microspheres/mL, 100 μl injection, Molecular Probes) was sonicated, vortexed, and injected into the left ventricle of 12-instrumented anesthetized mice with a syringe. Five minutes after the injection, mice were sacrificed, and mouse brains were immediately removed and quickly frozen in dry ice. Coronal sections of 50-μm thicknesses were cut on cryostat at −20°C and collected on glass slides. Sections were fixed by 4% paraformaldehyde (4% PFA), and counted whole fluospheres in each 250 μm sections on 10 brain section (Bregma +1.70 mm to -0.22 mm).

Fluoromyelin staining - Coronal sections of 12-μm thicknesses (bregma +0.86 mm to +0.50 mm) were cut on cryostat at −20°C and collected on glass slides. Sections were fixed by 4% PFA, and rinsed three times in PBS, then permeabilize them in PBT (PBS + 0.2% Triton X-100) for at least 20 minutes. The sections were incubated with FluoroMyelin Green fluorescent myelin stain (1:300, Molecular probes) for 20 minutes at room temperature. Semi-quantification of the intensity of fluoromyelin staining was conducted on 10x magnification images and viewed using a Nikon upright microscope. Intensity of fluoromyelin staining were analyzed by quantifying mean intensity of the entire field of view for 3 brain sections of each animal, using ImageJ analysis software with no thresholds set.

Western blotting - Tissue samples of corpus callosum and cell culture were dissected in Pro-PREPTM Protein Extraction Solution (Boca scientific). Samples were heated with equal volumes of SDS sample buffer (Novex) and 10 mM DTT 100 at 95 ∘C for 5 min, then each sample (20 μg per lane) was loaded onto 4–20%

2

Tris–glycine gels. After electrophoresis and transferring to polyvinylidene difluoride membranes (Novex), the membranes were blocked in Brockace (AbD serotec) for 60 min at room temperature. Membranes were then incubated overnight at 4 °C with primary antibodies against pCREB (1:3000, upstate), MBP (1:1000, Thermo scientific), HIF1α (1:3000, abcam), NG2 (1:3000), GST-pi (1:5000), or β-actin (1:10000, Sigma aldrich) followed by incubation with peroxidase-conjugated secondary antibodies and visualization by enhanced chemiluminescence (Amersham).

Spectral Domain Optical coherence Microscopy (SD-OCM) – After mouse brain was removed en bloc, it was subjected to post-fixation for over 24 hours in 4% PFA at 4°C. The, 1 mm of coronal section was prepared using brain matrix. SD-OCM is used to acquire high resolution 3D optical images analogue to ultrasound, relying on intrinsic difference in refractive index in tissue, such as myelin sheath and cell bodies. It is based on Low Coherence Interferometry: a broadband source, Super Luminescent Diode with a center wavelength of 1310nm and a bandwidth of 170 nm giving a axial resolution of 3.5 um in tissue, is split into two arms, namely the reference arm (containing only a mirror) and the sample one [5]. The spectral variations of the backscattered light is recorded by a line scan camera and thanks to Fourier relationship, is converted into the depth profile. In the sample arm, a 40x water immersion objective (NA 0.8) is used which gives a lateral resolution of 0.9 μm and an en-face field of view of 375 um x375 um. The sample is then translated to image a larger area, the Maximum Intensity Projection of each volume is processed, and then stitch together [6].

Spontaneous alternative Y-Maze Test - Y-maze cognitive test was conducted between 7:00 AM to 9:00 AM. The maze consists of 3 arms (40 cm long, 9.5 cm high, and 4 cm wide, labeled arm-A, -B, or -C) diverging at a 120° from the central point. Experiments were performed in a dimly illuminated room, and the maze was cleaned with super hypochlorous water-soaked paper for discrimination of smell to avoid olfactory cues after every session. Mouse was placed at the center of the start arm and allowed to move freely through the maze in a 10-minute session without reinforcers such as food, water, or electric foot shock. This task was videotaped with a Victor camera (Everio GZ-MG-77-S) and the sequence of arm entries manually recorded in a blinded manner. An actual alternation was defined as entities into all the 3 arms on consecutive (eg. ABC, CAB, or BCA but not BAB). The maximum alternation was subsequently calculated by measuring the total number of arm entries minus 2 and the percentage of alternation was calculated as [actual alternation/maximum alternation] x100%. The total number of arms entered during the sessions was shown as locomotor activity.

5-Bromodeoxyuridine labeling - A cell proliferation marker 5-bromodeoxyuridine (BrdU from Sigma-Aldrich) was dissolved in saline. To observe newly generative cells, mice were intraperitoneally injected (50 mg/kg, BrdU) three times a day with 4-hour interval. Then, the mice were sacrificed within 2 hours from the last BrdU injection. To detect cell differentiation, mice were intraperitoneally injected (50 mg/kg, BrdU) three times a day with 4-hour interval. The mice were sacrificed 7 days after the BrdU injection.

Immunohistochemistry - Mouse brain was removed immediately *en bloc* and postfixed for 24 h in 4%

3

paraformaldehyde (4% PFA) in phosphate-buffered saline (PBS) at 4°C before cryoprotection by bathing in 30% sucrose. The brain was then frozen and 16-μm-thick consecutive coronal sections of the white matter were prepared using a cryostat. Brain sections were incubated at 37°C for 30 min in 1N HCl to detect BrdU labeling. Sections were incubated overnight with anti-BrdU (1:50; Oxford Biotechnology). Double immunofluorescence staining was performed by simultaneously incubating the sections overnight at 4°C with anti-GST-pi (1:200, MBL), anti-CNPase (1:100, abcam), anti- NG2 (1:100; chemicom), anti-PDGFR-α (CD140a, 1:200, BD phamamigen), anti-ssDNA (1:100, abcam), phospho-CREB (pCREB, 1:100, Cellsignaling), anti-Iba-1 (1:100, Wako), and anti-GFAP (1:200, Dako) antibodies. For double labeling, the primary antibodies were detected with Rordamine- or fluorescein isothiocyanate-conjugated secondary antibody (1:200; Jackson Immunoresearch Laboratories) after incubation for 1 h at room temperature. Subsequently, the slides were covered with VECTASHIELD mounting medium with DAPI (Vector Laboratories). Immunostaining was analyzed with a fluorescence microscope (Olympus BX51) interfaced with a digital charge-coupled device camera and an image analysis system.

Cell counting for brain sections - An investigator blinded to the experimental groups counted the number of stained cells in lateral side of corpus callosum (0.25 mm^2) of GST-pi-, NG2-, GFAP-, Iba-1- and pCREB-stained section and in the corpus callosum of three predefined BrdU, and ssDNA sections (bregma +1.18 mm, +0.98 mm, and +0.74 mm).

Cell culture - OPCs were prepared according to our previous work [7]. Briefly, cerebral cortices from 1- to 2-d-old Sprague Dawley rats were dissected, minced, and digested. Dissociated cells were plated in poly-D-lysine-coated 75 cm^2 flasks, and maintained in DMEM containing 20% heat-inactivated fetal bovine serum and 1% penicillin/streptomycin. After the cells were confluent (~10 days), the flasks were shaken for 1 h on an orbital shaker (220 rpm) at 37°C to remove microglia. They are then changed to new medium and shaken overnight (~20 h). The medium was collected and plated on noncoated tissue culture dishes for 1 h at 37°C to eliminate contaminating astrocytes and microglia. The nonadherent cells were collected and replated in Neurobasal medium containing glutamine, 1% penicillin/streptomycin, 10 ng/ml PDGF, 10 ng/ml FGF, and 2% B27 supplement (NB medium) onto poly-DL-ornithine-coated plates. Four to five days after plating, the OPCs were used for the experiments. To differentiate OPCs to myelin basic protein-positive oligodendrocytes, the culture medium was switched to DMEM containing 1% penicillin/streptomycin, 10 ng/ml CNTF, 50 ng/ml T3, and 2% B27 supplement. To mimic chronic mild-hypoxic condition, OPCs were incubated with non-lethal cobalt chloride ($CoCl_2$ from Sigma). Cilostazol and Rp-cAMP (both from Sigma) were dissolved in dimethysulphoxide. The final concentration of dimethysulphoxide in the culture medium was less than 0.1%, which had no effects on OPC survival and function. Cytotoxicity was assessed by lactate dehydrogenase (LDH) assay (Roche) according to the manufacture's instruction.

Immunocytochemistry - After cells reached 70–80% confluence, they were washed with ice-cold PBS (pH 7.4), followed by 4% PFA for 15 min. After being further washed three times in PBS containing 0.1% Triton

4

X-100, they were incubated with 1% bovine serum albumin in PBS for 1 h. Then cells were incubated with primary antibodies against NG2 (1:200), MBP (1:100, abcam), GST-pi (1:100), CNPase (1:100), PDGFR-α (1:200) and pCREB (1:100) at 4°C overnight. After washing with PBS, they were incubated with secondary antibodies for 1 hour at room temperature. Finally, nuclei were counterstained with DAPI.

Statistical analysis - Based on published and pilot data, power estimates were calculated based on α=0.05 and β=0.8 to obtain group sizes appropriate for detecting effect sizes in the range of 30-50% for in vivo models and 40-50% for cell cultures models. A one-way ANOVA followed by post-hoc Fisher-protected least significant difference test was used to determine the significant differences in various indices among the groups. A p-value of <0.05 was considered statistically significant.

Supplemental Table:

**Supplementary Table 1: Cell types of BrdU-positive cells (%).**

		NG2	GST-pi	GFAP
pretreatment	2-month old	90.7 ± 6.5	3.1 ± 6.3	2.5 ± 4.3
	8-month old	91.6 ± 6.7	3.2 ± 4.3	3.1 ± 4.1
day 3	2-month old	87.7 ± 8.8	2.1 ± 4.0	21.7 ± 4.1
	8-month old	84.6 ± 10.9	2.5 ± 6.3	18.8 ± 14.2
day 7	2-month old	90.1 ± 2.4	3.3 ± 4.0	3.3 ± 4.1
	8-month old	92.1 ± 6.8	3.1 ± 6.3	2.5 ± 5.0
day 14	2-month old	95.0 ± 4.5	5.2 ± 6.3	5.2 ± 6.3
	8-month old	90.9 ± 6.3	3.6 ± 7.1	3.1 ± 5.4

NG2; a marker for OPCs, GST-pi; a marker for mature oligodendrocytes, GFAP; a marker for astrocytes,
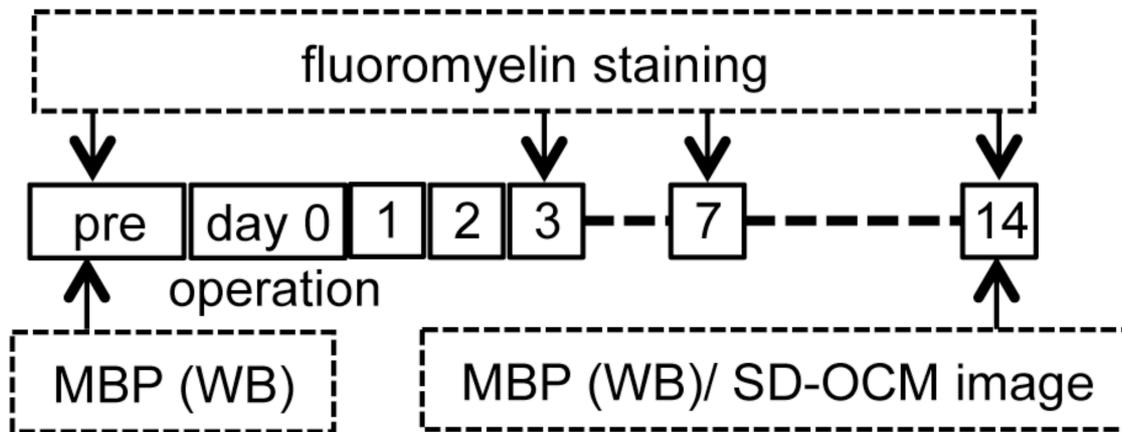
Values are mean +/- SD of 5 mice in each group.

Supplementary Figure 1:

Representative images of fluolomyelin staining in mouse corpus callosum. Bar= 100 μm. 2M: 2-month old mouse, 8M: 8-month old mouse.
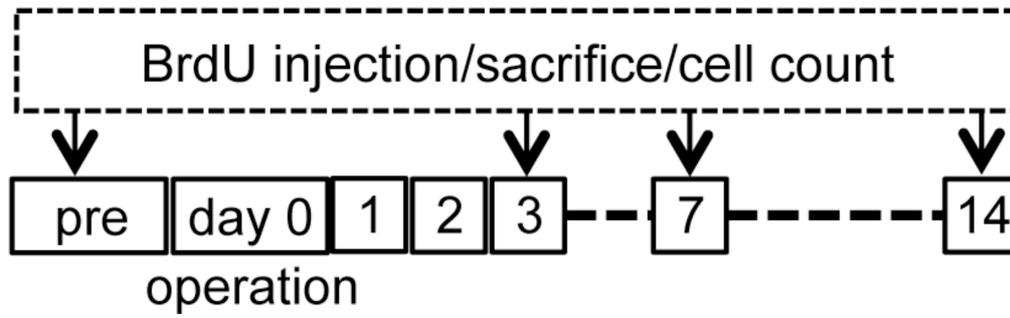

7
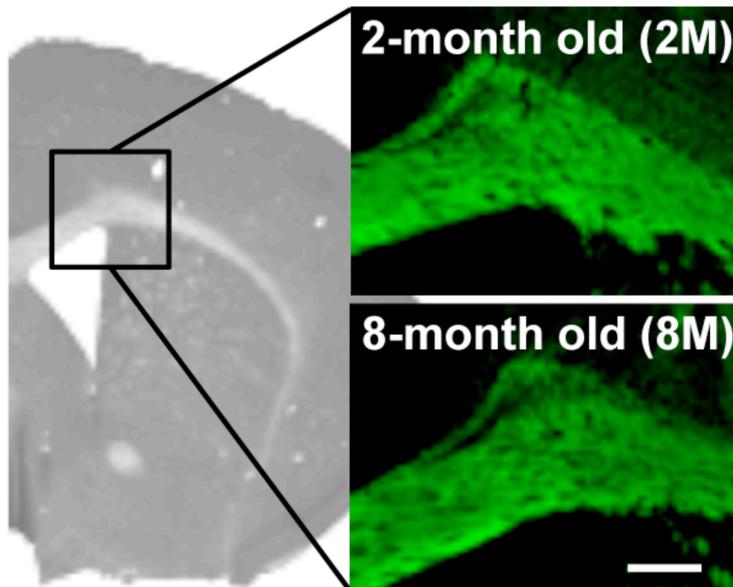
Supplementary Figure 2:

Experimental schedules to assess white matter integrity during hypoperfusion stress.

Supplementary Figure 3:

Experimental schedule to assess newly generated cells in the corpus callosum using BrdU.

Supplementary Figure 4:

Distribution data of pCREB in OPCs and OLs under normal conditions. Immunostaining analyses showed that, both in young (2M) and older (8M) white matters, phosphorylated CREB signaling was observed in mature OLs (CNPase-positive) as well as OPCs (PDGF-R-α-positive). But importantly, phosphorylated CREB was primarily expressed within OPCs. 2M: 2-month old mouse, 8M: 8-month old mouse.
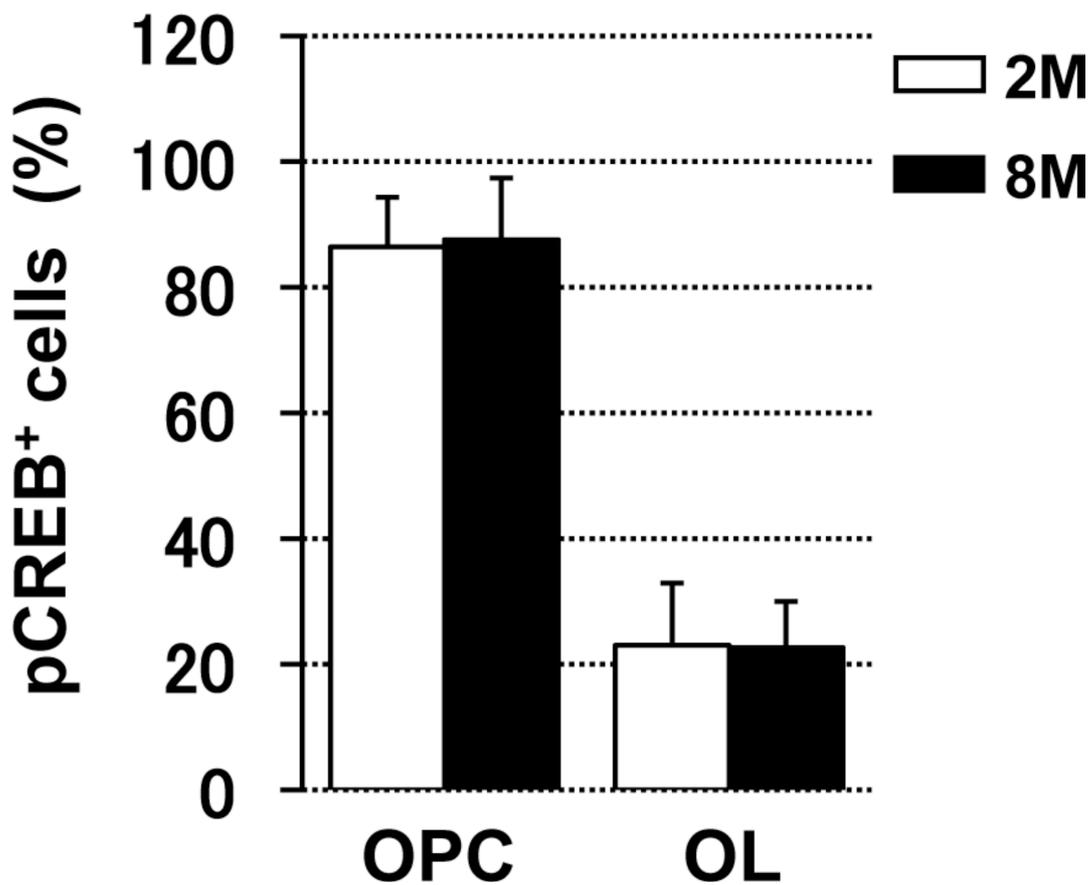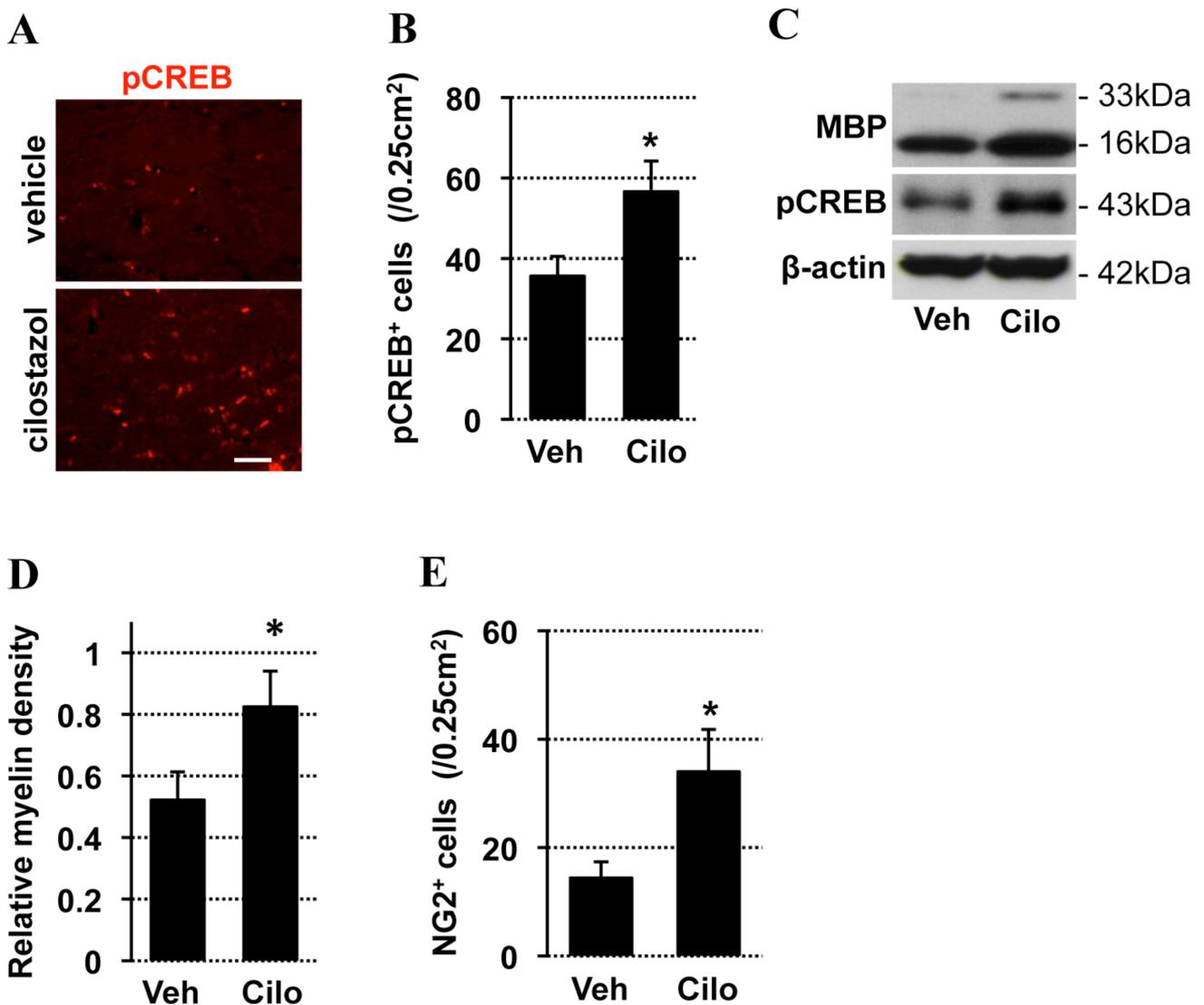
Supplementary Figure 5:

Western blot images using samples from cultured rat OPCs with 7-day CoCl2 treatment with or without cilostazol. HIF1α is a marker for hypoxic conditions, NG2 is a marker for OPCs, GST-pi and MBP are markers for mature oligodendrocytes, and β-actin is an internal control.


11
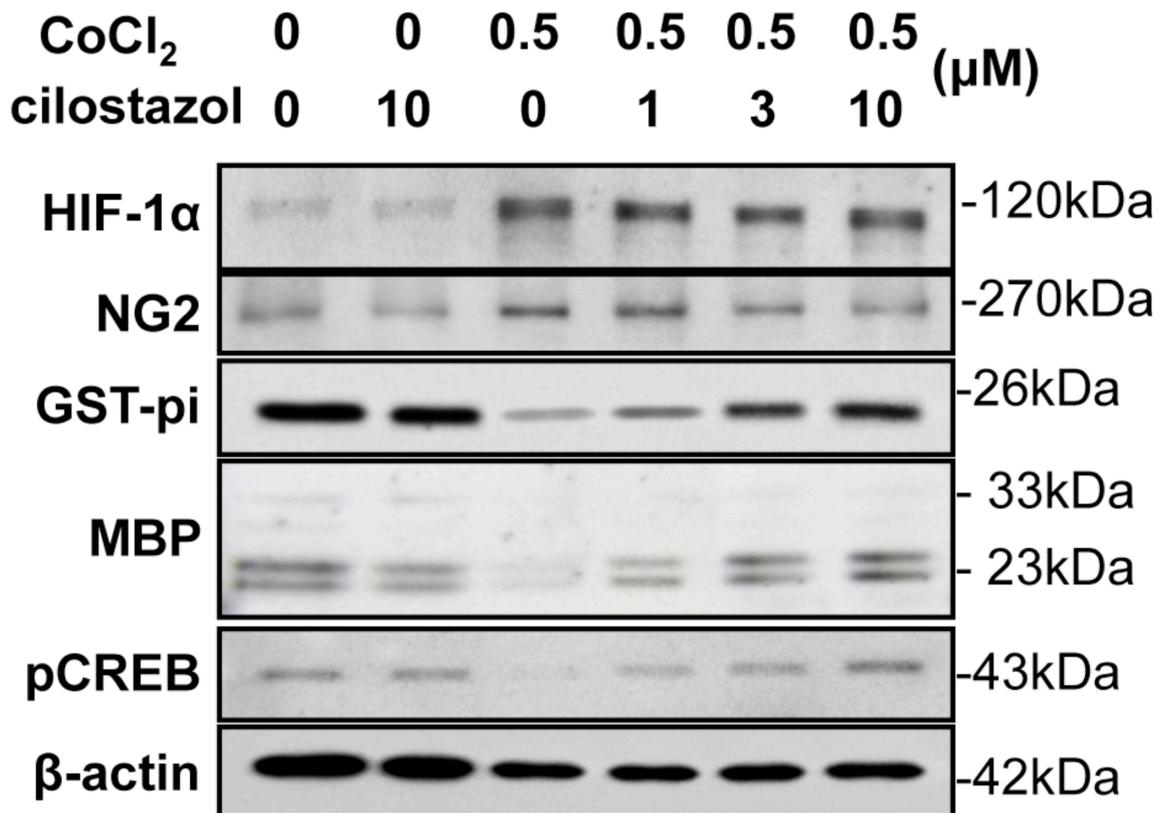
Supplementary Figure 6:

A. CREB phosphorylation in the lateral side of corpus callosum with or without cilostazol (10 mg/Kg/day for 14 days, i.p.) in 8-month old mice at day 14 after the white matter injury. Bar = 25 μm. **B.** Number of pCREB-positive (pCREB$^+$) cells in the lateral side of corpus callosum at day 14. N=5. **C.** Western blot images of MBP and pCREB expressions in corpus callosum at day 14. β-actin is an internal control. **D.** Relative density of fluolomyelin intensity in corpus callosum at day 14. Values were calculated based on the density of pretretment in 2-month old mice. N=5. Representative images of fluolomyelin are shown in Fig 6A. **E.** Number of NG2–positive (NG2$^+$) cells in the lateral side of corpus callosum in 8-month old mice at day 14. N=5. Representative images of NG2 staining are shown in Fig 6B.


12

Supplementary Figure 7:

Experimental schedule to assess cell differentiation in the corpus callosum in 8-month old mice using BrdU.

13
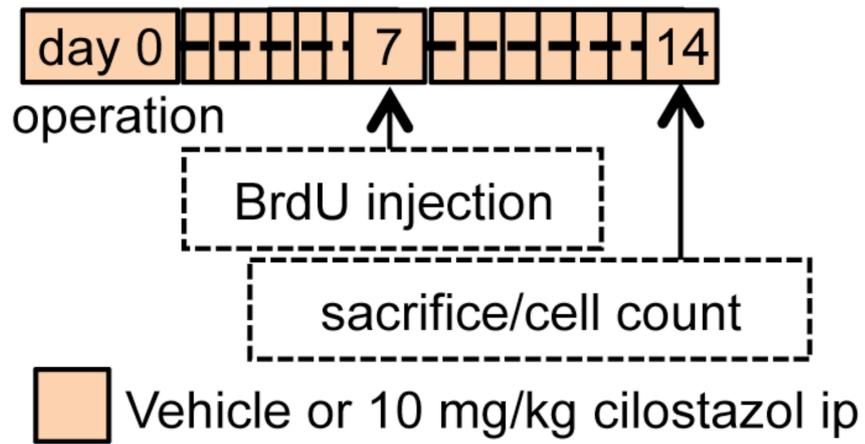
Supplementary Figure 8:

A. Representative images of BrdU staining in the corpus callosum in 8-month old mice with or without cilostazol at day 14. Bar = 100 μm. Experimental schedule for these experiments is shown in Supple Fig S6. **B.** Number of BrdU positive cells (BrdU[+]) in the corpus callosum in 8-month old mice with or without cilostazol at day 14. N=5. Values are mean ± SD. *$P<0.05$.

14
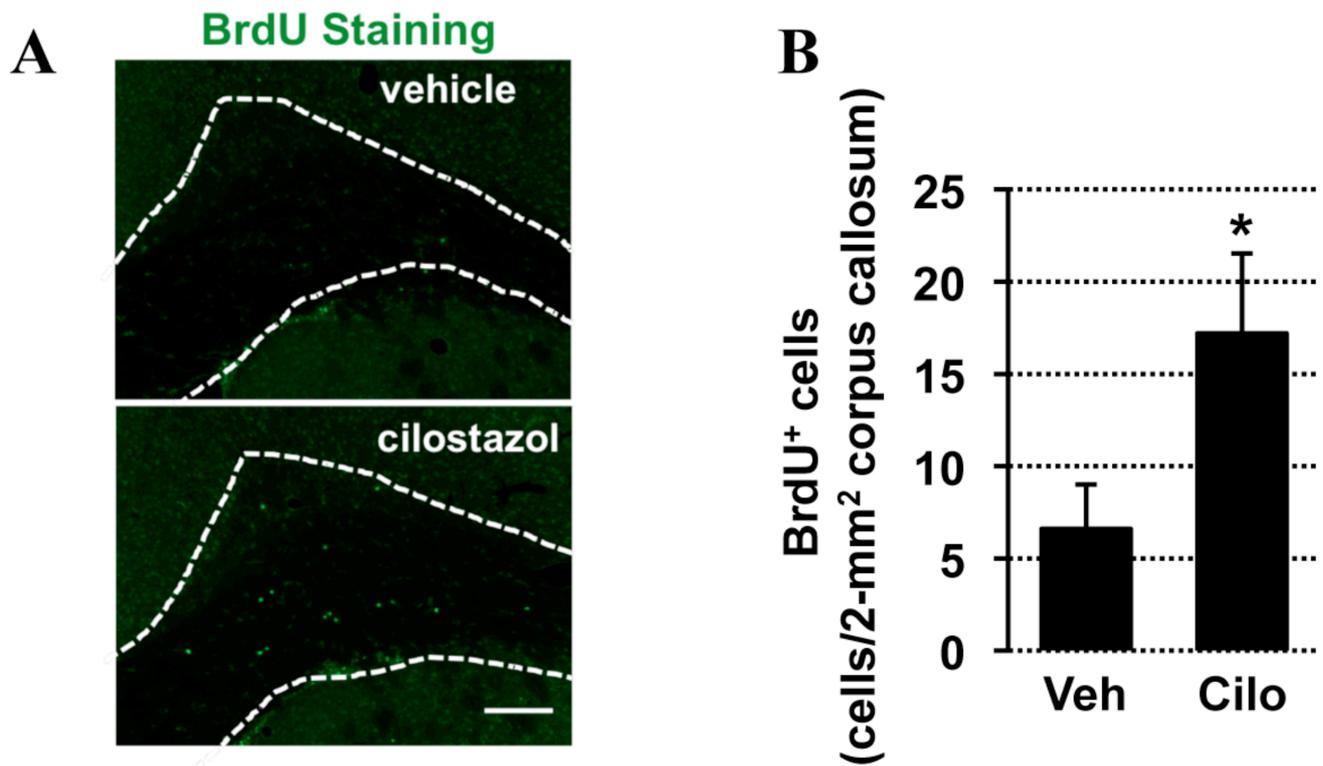
Supplemental References:

1.   Zarember KA, Malech HL. Hif-1alpha: A master regulator of innate host defenses? *J Clin Invest.* 2005;115:1702-1704

2.   Harris AL. Hypoxia--a key regulatory factor in tumour growth. *Nat Rev Cancer.* 2002;2:38-47

3.   Siddiq A, Ayoub IA, Chavez JC, Aminova L, Shah S, LaManna JC, et al. Hypoxia-inducible factor prolyl 4-hydroxylase inhibition. A target for neuroprotection in the central nervous system. *J Biol Chem.* 2005;280:41732-41743

4.   Shibata M, Ohtani R, Ihara M, Tomimoto H. White matter lesions and glial activation in a novel mouse model of chronic cerebral hypoperfusion. *Stroke.* 2004;35:2598-2603

5.   Srinivasan VJ, Radhakrishnan H, Jiang JY, Barry S, Cable AE. Optical coherence microscopy for deep tissue imaging of the cerebral cortex with intrinsic contrast. *Opt Express.* 2012;20:2220-2239

6.   Preibisch S, Saalfeld S, Tomancak P. Globally optimal stitching of tiled 3d microscopic image acquisitions. *Bioinformatics.* 2009;25:1463-1465

7.   Arai K, Lo EH. An oligovascular niche: Cerebral endothelial cells promote the survival and proliferation of oligodendrocyte precursor cells. *J Neurosci.* 2009;29:4351-4355

15